Thermally chained LES of a GCH4/GOX single element combustion chamber

By D. Maestro, L. Selle†, AND B. Cuenot‡

CERFACS - Centre Européen de Recherche et de Formation Avancée en Calcul Scientifique, 42 Avenue Gaspard Coriolis, 31057 Toulouse Cedex 01, France

A large eddy simulation of the single element GCH4/GOX combustion chamber characterized at TUM has been performed in this work, followed by a chained calculation of the chamber structure temperature distribution using the heat fluxes provided by the LES. The strong dependency of this configuration to the mesh characteristics, and especially to the post-tip resolution, has been investigated and flow and flame characteristics for two different meshes have been presented. It is shown how an insufficient number of grid points in the post-tip zone does not permit to retrieve the close-injector recirculation zone and leads to big recirculation zones downstream, pushing the CH4 jet towards the walls (reducing the dimension of corner recirculation zones) and to a different flame shape. Computed data of pressure along the chamber walls and of temperature in the solid structure have been compared with experimental data. A linked effect of pressure underestimation and temperature (wall fluxes) overestimation is found and is the subject of ongoing study and further work.

1. Introduction

In the liquid rocket engine community a large number of studies are devoted to the use of methane and oxygen as propellants because of several advantages that methane presents if compared with hydrogen or others storable propellants. Moreover, particular attention is given to two critical aspects in the design of the combustion chamber: (1) injector technology and (2) heat transfer evaluation.

At present time little experimental data is available at relevant combustion chamber conditions and numerical simulations, which allow to understand the physics of such reacting flows, are of high interest.

In this context, an experimental test campaign has been carried out at TUM (Technische Universität München) in the framework of the national research program Transregio SFB/TR-40. Different gaseous oxygen (GOX) / gaseous methane (GCH4) combustion chambers have been built to study heat transfer and film cooling at high pressures, while testing optical measurement techniques.

As a first step of study, a shear coaxial single-element injector has been built and tested [1, 2]; pressure evolution in the chamber has been measured through pressure transducers in the chamber wall and wall heat transfer characteristics have been documented through measures of temperature in the chamber structure. This chamber is

† IMFT - Institut de Mécanique des Fluids de Toulouse
‡ also at CERFACS

Pressure	O/F ratio	Mass flow rate GOX	Temperature GOX	Mass flow rate GCH4	Temperature GCH4
20 bar	2.6	0.045 kg/s	278 K	0.017 kg/s	269 K

TABLE 1. Operational parameters

used for the validation of numerical tools, and the data provided by TUM will be here compared with numerical simulations.

Large Eddy Simulation (LES) coupled with the heat transfer by conduction in the wall material provides a suitable approach to simulate this experiment. For this purpose, the flow solver AVBP, developed by CERFACS-IFPEN, and the thermal solver AVTP are used. The present research work focuses on the LES of the TUM experiment, followed by a chained calculation of the temperature distribution in the chamber structure.

The paper is organized as follows: in section 2 the experimental setup is shortly presented, section 3 is dedicated to a description of the simulation methodology, LES and thermal simulation numerical setup are summarized in section 4 and 5, flow and flame structure and mesh improvement are described in section 6 and quantitative results for the LES and thermal calculation are detailed in section 7. Finally, conclusions and future work are summarized in section 8.

2. Reference experiment

In this section only the key characteristics of the reference experiment facility are reminded and the reader is referred to [3] for a detailed description.

The experimental setup consists of a single coaxial injector combustion chamber, operating in the 20 bar pressure range. The shear coaxial injector is flush mounted on an oxygen-free copper combustion chamber with a square cross section and a nozzle at the exit, which is schematically reported in Fig. 1 together with a detail of the injector. Operating experimental conditions are known at the inlet in terms of temperature and pressure. Operational values are reported, together with mass flow rates, in Tab. 2.

The test case is instrumented with pressure transducers and thermocouples all along the chamber. No cooling system is present and therefore the wall chamber temperature increases during the burning experimental time, which is 3 s. The measured wall temperature in the chamber is thus averaged over a shorter evaluation time of 0.5 s, centered at 2/3 of the burning time, and is used as boundary condition for the numerical simulation as will be detailed in section 7.

3. Computational methodology

The proposed approach is to numerically reproduce the experimental conditions in the present test case with a 3D LES of the flow field, starting in the nozzle, 1 mm before the faceplate, until the nozzle exit. Experimental conditions will be assigned in terms of propellant mass flow rates and temperature. Furthermore, the effect of the thermal coupling will be considered, both in the chamber and at the injector lip. Specifically, the goals of the project are:

(*a*) To carry out a LES computation, by assigning the experimental temperature profile (variable in space) at the chamber walls with an isothermal boundary condition. The

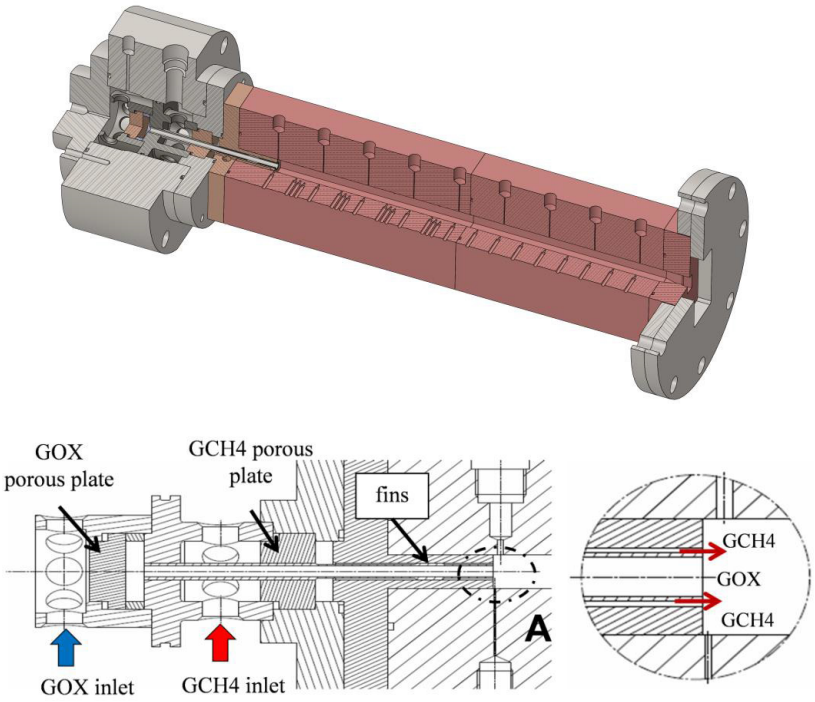

FIGURE 1. Single injector combustion chamber and detail of the injector

isothermal boundary assumption can be made because the convective time, evaluated from the propellant velocities (about 2.7 ms), is low enough to ensure a decoupling between the wall chamber temperature evolution, which is averaged over 500 ms in the experimental data, and the flow field. The expected results are the pressure evolution, that will be compared with the experimental data and the wall heat flux profile. A similar calculation with the AVBP solver can be found in [4].

(*b*) To impose the computed heat flux as a boundary condition for the thermal solver (AVTP), assuming that it remains constant over the duration of the test. This will provide the temporal temperature evolution within the solid.

4. Large eddy simulation setup

4.1. *Geometry - Computational domain and Mesh characteristics*

For the LES simulation, the computational domain is the full three-dimensional chamber and starts 1 mm before the faceplate, so that just a small part of the injector is calculated. On the other side, the computational domain ends at the nozzle exit and the full nozzle is simulated.

The computational domain is discretized with a fully tetrahedral unstructured mesh of about 50 millions cells. Particular attention has been put on the flame zone refinement, especially in the post-tip zone, which has been discretized with 20 cells. As will be shown in section 6, the post-tip resolution is crucial to retrieve correct flow characteristics. Mesh characteristics are summarized in Tab. 2.

Type	Cell type	Number of cells	Smaller cell volume	Post-tip resolution
Unstructured	Tetrahedral	50 M	$6.7 \cdot 10^{-16}$ m^3	20 cells

TABLE 2. Mesh parameters

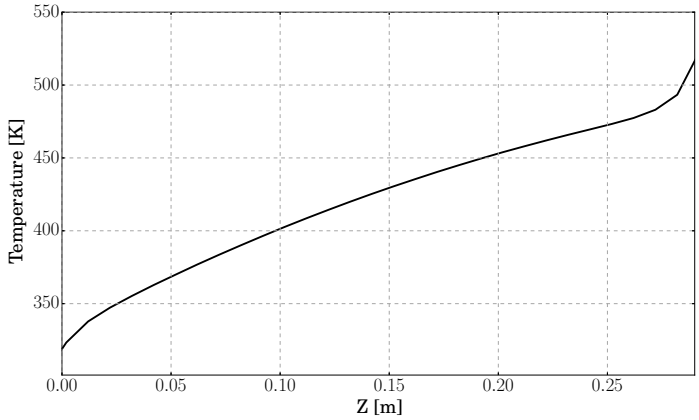

FIGURE 2. Experimental temperature profile used for imposed temperature boundary condition at the chamber walls

4.2. *Boundary conditions*

At the inlets GOX and GCH4 mass flow rates are prescribed, as well as the measured temperature, using the NSCBC formulation [5], while at the outlet the flow is expected to be supersonic, therefore there is no need to specify a boundary condition. The velocity profile used at inlet is a flat "infinitely turbulent" profile, without turbulent fluctuations. The injectors walls, as well as the faceplate, post-tip and nozzle walls are treated as slip adiabatic walls. Chamber walls are modeled with isothermal wall laws, using an improved formulation that couples the velocity and temperature profiles to take into account the interaction between the strong temperature and density gradients in the boundary layer. A detailed description of this coupled wall law can be found in [6]. The imposed temperature profile is taken from [3]; the values have been averaged between the ones provided on the upper and lateral walls and the same profile has been imposed on the four walls. The imposed temperature profile is plotted in Fig. 2.

4.3. *Numerical setup*

The AVBP solver, developed by CERFACS and IFPEN, is used to carry out the LES. It is an unstructured, explicit, compressible code, which relies on the cell-vertex and finite-volume methods [7, 8]. Among others, the code has a two step Taylor-Galerkin scheme, TTGC, which is third order in space and time [9]. The subgrid stress tensor are closed with the Smagorinsky model [10], which has been validated as the best available option in combination with wall laws. Thermal and species diffusion terms are deduced assuming an eddy diffusivity approach assigning constant turbulent Prandtl number and turbulent Schmidt number (value fixed at 0.6 for both). Regarding turbulence/combustion interaction, the flame/eddies interaction is fully resolved and no additional model is needed.

4.4. *Chemistry*

The solver accounts for multi-species thermodynamics and transport. In particular, under the present experimental conditions perfect gas thermodynamic models can be applied. Particular attention must be given to the chemical mechanism employed to describe the CH4/O2 combustion. The 13 species (CH4, O2, CO2, CO, H2O, N2, H2, H, OH, O, HO2, CH3 and CH2O), 73 elementary reactions semi-analytic mechanism of Lu [11] has been implemented into AVBP and has demonstrated the ability to correctly reproduce equilibrium conditions, flame speed, etc. in various conditions [12].

Due to the stiffness of the chemistry model, sub-cycling was implemented for the calculation of the chemical source term. For one CFL time step, ten chemical time steps are calculated.

5. Thermal simulation setup

The thermal simulation has been performed by means of the AVTP solver, dedicated to conduction in solids. AVTP solves the time dependent temperature diffusion equation, where the heat diffusion follows Fourier's law. The solid solver takes into account local changes of heat capacity and conductivity with temperature. The second order Galerkin diffusion scheme [13] for spatial discretization is derived from the AVBP solver. Time integration is achieved either with an explicit or an implicit first order forward Euler scheme. The implicit system, which has been used in the present study, is solved with a parallel matrix free conjugate gradient method [14].

The whole chamber structure has been calculated, starting from 29 mm before the faceplate until the end of the nozzle, and has been discretized by means of a fully tetrahedral unstructured mesh of about 33 millions of cells. The structure material is oxygen-free copper (Cu-HCP), with the characteristics provided in [3], which have been considered constant with temperature.

The computational domain has been initialized with a constant temperature of 293 K and the following boundary conditions have been used:

– heat fluxes (constant in time and variable in space) from the large eddy simulation for the four chamber walls,

– isothermal walls for the faceplate and the external GCH4 injector wall, both fixed to the experimental chamber wall temperature at the faceplate axial coordinate,

– isothermal walls for the nozzle walls, fixed at the experimental chamber wall temperature at the last chamber wall axial coordinate,

– heat loss for the structure external walls, considering an air temperature of 293 K (the same as the initial temperature of the structure) and an arbitrary convective heat transfer coefficient of 15 W/m^2K.

The entire period of three seconds of the experiment have been simulated.

6. Flow and flame structure - Mesh improvement

In such configuration the physical mechanisms which are present just downstream of the post-tip have been found to strongly govern the flow and flame structure in the close injector region, and a process of analysis and improvement of the mesh resolution was necessary to ensure a correct solution.

Flow and flame structure are presented for both a coarse mesh, where the post-tip zone is discretized with 10 points, and for a fine one (which is the one used for the

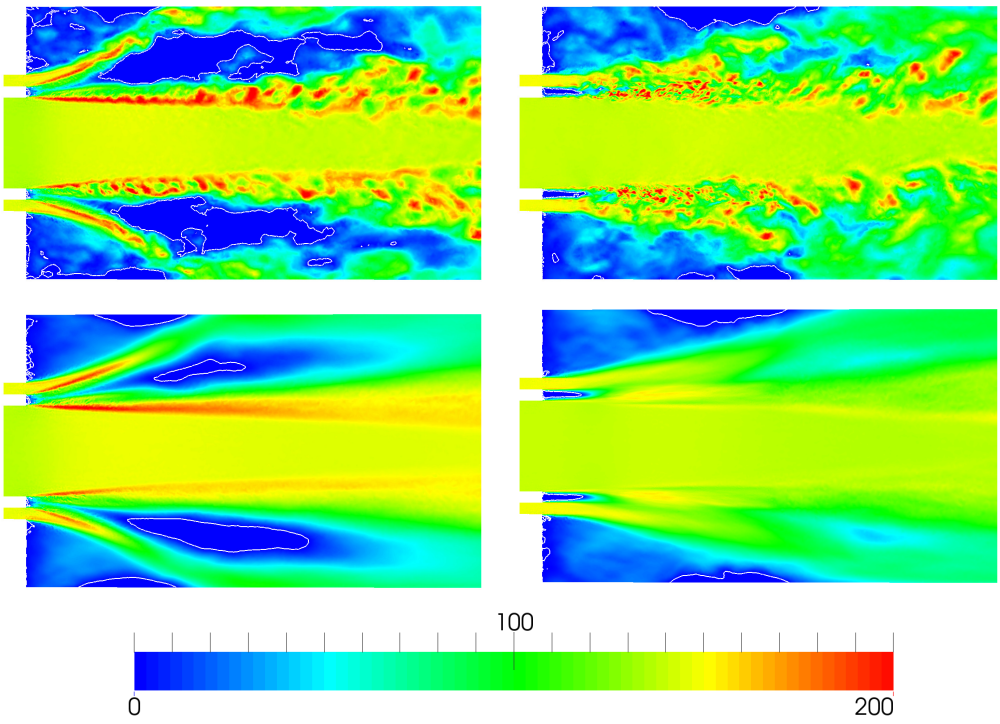

FIGURE 3. Fields of axial velocity downstream of the faceplate in the middle plane. Top: instantaneous fields; Bottom: averaged fields. Left: coarse mesh; Right: fine mesh. Isolines of zero axial velocity are plotted in white.

rest of the work), where the post-tip zone is discretized with 20 points. All the other mesh parameters have been kept constant. As shown below, this difference, although moderate, changes completely all the flow and flame structure downstream of the post-tip.

Figure 3 shows the flow structure by means of instantaneous and averaged axial velocity fields for the two meshes (coarse mesh at left side and fine mesh at right side). It can be seen that different recirculation zones appear, depending on the mesh used: a "tip recirculation zone" (fine mesh) in the post-tip zone, two "central recirculation zones" (coarse mesh) a little further downstream and "corner recirculation zones" in the chamber corners (both meshes). One can immediately notice how, due to the too coarse mesh, the "tip recirculation zone" almost disappears, and just a track of it remains. On the contrary, this recirculation zone, filled with hot burned gases, is well retrieved with the fine mesh and Fig. 3 (right) shows how its presence is crucial for the flow structure just downstream: the reactant jets are pushed closer by this vortical structure, they mix and do not leave place for any "central recirculation zone".

This phenomenon modifies the flame structure, as shown by Fig. 4, where instantaneous and averaged temperature fields are presented: in the case of a coarse mesh the flame is less strained and the hot products are free to expand radially, while in the case with a fine mesh the flame stays very thin. This flame structure difference has in turn an impact on the flow structure: through radial expansion, the thick flame on the

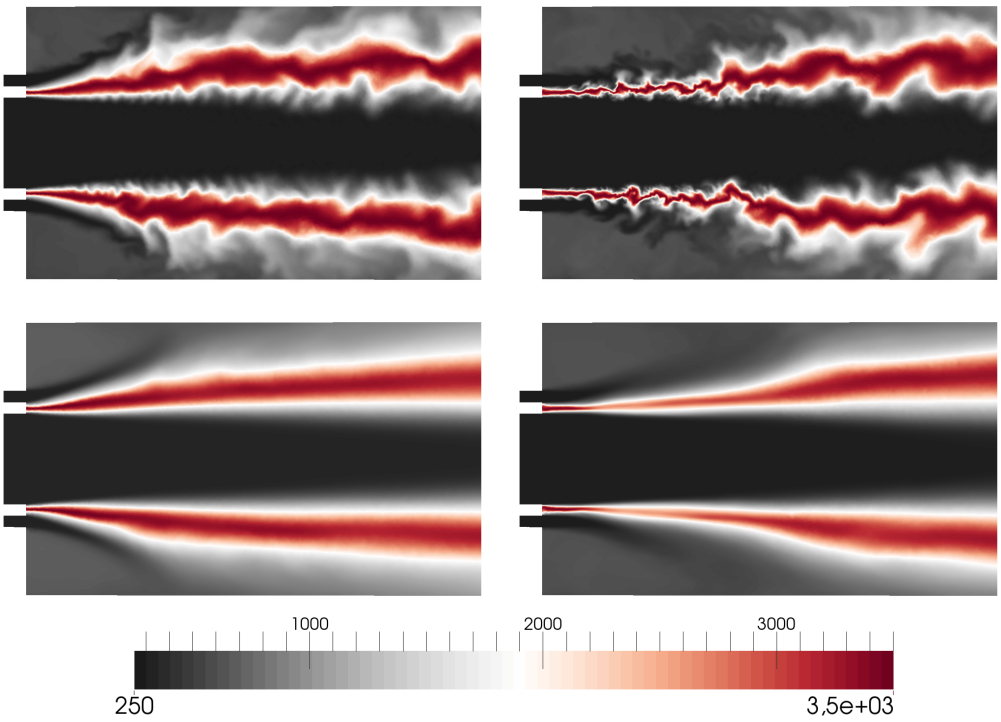

FIGURE 4. Fields of temperature downstream of the faceplate in the middle plane. Top: instantaneous fields; Bottom: averaged fields. Left: coarse mesh; Right: fine mesh.

coarse mesh pushes the CH4 jet toward the chamber walls, while the thin flame on the fine mesh does not lead to sufficient expansion to modify the flow. The jet breakdown position coincides in this case with a slowdown zone, but no back flow is observed.

This has a direct effect on the "corner recirculation zone" length, which changes from 9 mm with the coarse mesh to 14 mm with the fine mesh.

The flow structure downstream the post-tip has a direct influence on the flame stabilization mechanism. Figure 5 shows a zoom on the heat release rate field in post-tip zone for both cases. With the coarse mesh the reactants quickly diffuse immediately after the post-tip creating favorable conditions for combustion and leading to a maximum of heat release. On the contrary, with the fine mesh, the recirculation zone (marked by isolines of zero axial velocity, in white) confines the flame on the oxygen side and dilutes the CH4 flux with burned gases, limiting the heat release which reaches its maximum later downstream.

In Fig. 5, isolines of stochiometric mixture fraction are also plotted in black. For the coarse mesh the expected alignment with the heat release zone immediately at the post-tip is observed, confirming that the flame burns as a pure CH4/O2 diffusion flame. Conversely, with the fine mesh, the alignment arrives later, in the region where CH4 is not anymore diluted with burned gases.

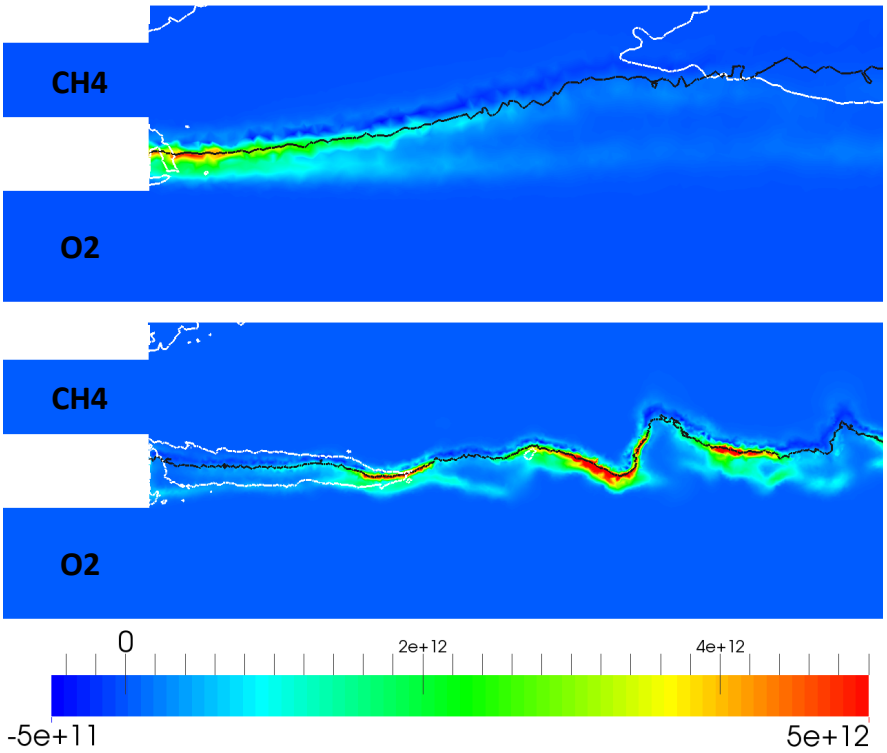

FIGURE 5. Zoom on the post-tip zone. Fields of instantaneous heat release rate; isolines of stochiometric mixture fraction in black and isolines of zero axial velocity in white. Top: coarse mesh; Bottom: fine mesh.

7. Comparison with experiment

Quantitative results are here presented for the LES and for the thermally chained simulation. The pressure evolution on the chamber wall and the solid temperature in the chamber structure are compared with the experiment. The pressure evolution along the chamber wall is plotted in Fig. 6 (top), while in the bottom figure a non-dimensional value is shown, where the local pressure value was divided by the numerical value at the last transducer position, as was done in the experiment.

Figure 6 shows how pressure is globally underestimated, probably due to an overestimation of heat losses at walls, as is shown in the following. However, the global trend is well captured and in particular one can notice:

– a peak in the immediate vicinity of the faceplate denoting the end of the "corner recirculation zone" and the impact of the flow to the wall. The peak seems to be estimated a little earlier in the simulation than in the experiment, denoting a slightly shorter recirculation zone than in reality,

– a gradual decay in the flame zone due to flow acceleration,

– a plateau (low pressure gradient) in the zone close to the end of the chamber, denoting the end of the combustion process.

Regarding the solid, results at the evaluation time (see [3] for further information) are presented in Fig. 7, where the evolution of the chamber temperature is plotted versus the axial coordinate. Computed values are here compared with the experimental data

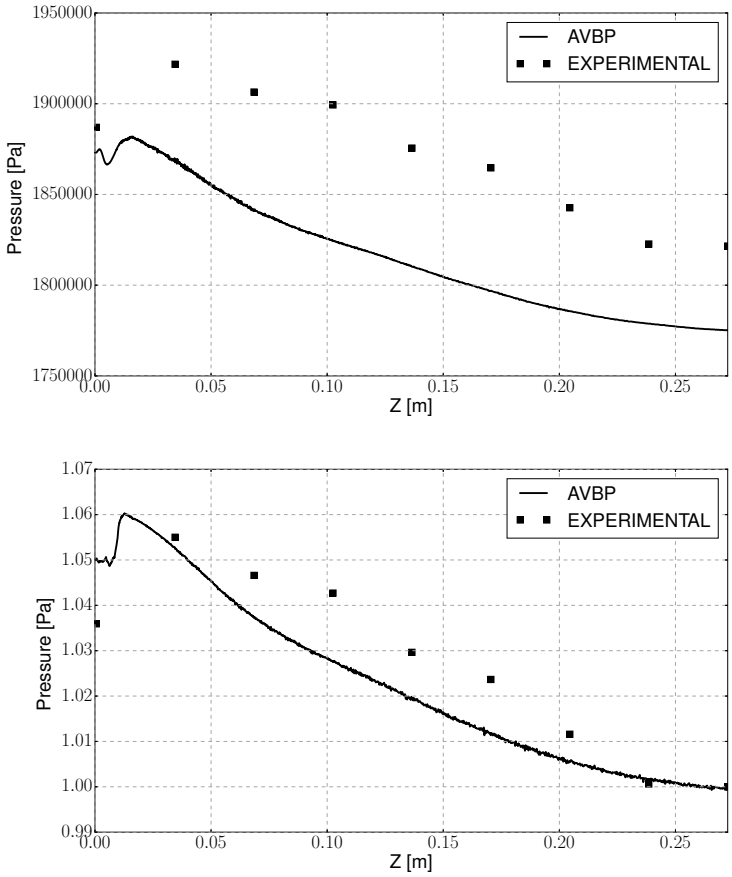

FIGURE 6. Pressure evolution along the chamber wall (top) and non-dimensional pressure evolution (bottom).

recorded for the series of thermocouples mounted at a distance of 1 mm from the chamber wall.

Figure 7 shows how the solid temperature is generally overestimated, due to an overestimation of the wall heat fluxes in the LES. One can notice two different but linked effects: first an overshoot in temperature is present, denoting temperatures in the fluid higher than the expected ones close to the walls, due probably to a lack of resolution of the flow and flame shape downstream of the refined zone. Second, in the zone near to the end of the chamber, a slight overestimation of the temperature is visible, suggesting that even in zones with no strong flame/wall interaction the heat fluxes are overestimated. This is probably caused by the lack of resolution of the chamber walls boundary layer, that are treated with wall laws using values for y^+ around 600. This effect can in turn be in part the cause of the overestimation of the fluxes in the central part of the chamber, where really high differences in temperature appear in a not sufficiently refined zone.

Moreover it should be pointed out that the temperature is well predicted in the very first part of the chamber, denoting a correct estimation of the temperature and chemical

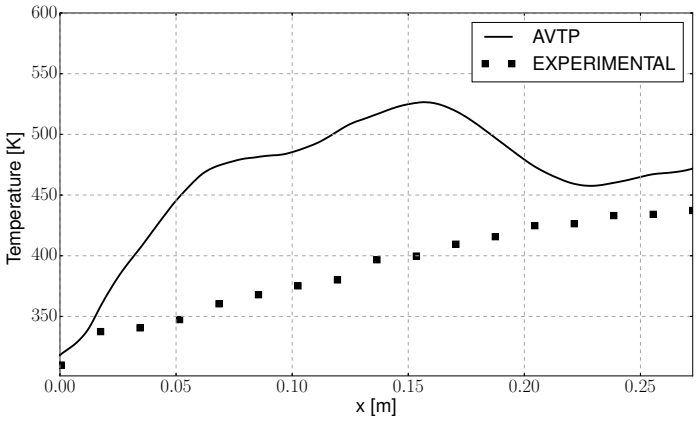

FIGURE 7. Temperature evolution along the 1 mm thermocouples line.

composition of the recirculation zone, which has been found to be filled with a mixture of fresh methane and hot burned gases brought back by the corner back flow.

All these effects are the subject of ongoing studies and future work.

8. Conclusions

In the present work a large eddy simulation of a single element coaxial GCH4/GOX combustion chamber has been performed, followed by a chained calculation of the heat transfer in the solid structure by means of the AVBP and AVTP solvers.

Regarding the LES, it has been shown how the configuration is extremely sensitive to the mesh characteristics downstream of the post-tip and how flow and flame structure can completely change for two different meshes. It has been found that, without a sufficient number of points, the "tip recirculation zone" is not correctly captured and this leads to large "central recirculation zones" downstream that push the CH4 jet towards the walls, changing the size of the "corners recirculation zones" and the heat release topology. The pressure along the chamber walls has been found to be underestimated, but the overall shape of its evolution with the axial coordinate is correctly retrieved.

The chained thermal calculation has been performed starting from heat fluxes of the LES, showing an overestimation of the predicted temperature in the first part of the chamber, due to an overestimation of the heat fluxes caused by a too coarse mesh in the boundary layer.

This linked effect of underestimation of chamber pressure and overestimation of chamber solid temperature, as well as the influence of the mesh on the flame structure and of the wall resolution on heat losses, is the subject of ongoing study and further work.

Acknowledgments

Financial support has been provided by the German Research Foundation (Deutsche Forschungsgemeinschaft – DFG) in the framework of the Sonderforschungsbereich Transregio 40. Computational resources have been provided by the High Performance Computing Center Stuttgart (HLRS) and by GENCI (Grand Equipement National de Calcul Intensif) under the allocation *x20152b5031*.

References

[1] CELANO, M., SILVESTRI, S., SCHLIEBEN, G., KIRCHBERGER, C. AND HAIDN, O. (2013). Injector characteristic for a GOX/GCH4 Single Element Chamber. *EUCASS conference*

[2] CELANO, M., SILVESTRI, S., SCHLIEBEN, G., KIRCHBERGER, C. AND HAIDN, O. (2014). Characterization of a a GOX/GCH4 Single Element Chamber. *Space Propulsion*

[3] CELANO, M., SILVESTRI, S., SCHLIEBEN, G., KIRCHBERGER, C. , KNAB, O. AND HAIDN, O. Transregio SFB-TR40 Test Case 1. Single Element Combustion Chamber GCH4/GOX. *Technical report*

[4] URBANO, A., SELLE, L., STAFFELBACH, G., CUENOT, B., SCHMITT, T., DUCRUIX, S., AND CANDEL, S. (2015) Large eddy simulation of a model scale rocket engine. *9th Mediterranean Combustion Symposium*

[5] POINSOT, T. AND LELE, S. (1992). Boundary conditions for direct simulations of compressible viscous flows. *J. Comput. Phys.*, **101**(1), 104–129.

[6] CABRIT, O (2009) Modelisation des flux parietaux sur les tuyeres des moteurs a propergol solide. *PhD thesis, INP Toulouse*

[7] SCHØNFELD, T. AND RUDGYARD, M. (1999) Steady and unsteady flows simulations using the hybrid flow solver avbp. *AIAA Journal* , **37**(11), 1378–1385.

[8] GOURDAIN, N.,GIQUEL, L., STAFFELBACH, G., DUCHAINE, F., BOUSSUGE, J.-F. AND POINSOT, T. (2009) High performance parallel computing of flows in complex geometries - part 2: applications. *Comput. Sci. Disc.* , **2**(1).

[9] QUARTAPELLE, L. AND SELMIN, V. (1993) High-order Taylor-Galerkin methods for nonlinear multidimensional problems. *Finite Elements in Fluids* , **76**(90), 46.

[10] SMAGORINSKY, L. (1963) General circulation experiments with the primitive equations, I. the basic experiment. *Monthly Weather Review* , **91**(3), 99–164.

[11] LU, T. AND LAW, C.K. (2008) A criterion based on computational singular perturbation for the identification of quasi steady state species: A reduced mechanism for methane oxidation with no chemistry. *Comb. and Flame* , **24**, 761–778.

[12] MARI, R (2015) Impact of conjugate heat transfer in liquid rocket engines. *PhD thesis, INP Toulouse*

[13] DONEA, J AND HUERTA, A. (2003) Finite Element Methods for Flow Problems. *John Wiley & Sons Inc, New York*

[14] FRAYSSÉ, V, GIRAUD, L., GRATTON, S. AND LANGOU, J. (2005) A set of GMRES routines for real and complex arithmetics on high performance computers. *ACM Trans. Math. Softw.*, **31**(2), 228–238